

Improving the structural performance of biomaterials through cellulose nanocrystal-reinforced polymer nanocomposites

Dr. A. Ibrahim¹, Dr. N. Hassan¹, Dr. S. Mahmoud¹, Dr. K. Farouk^{1*}

¹ Faculty of Medicine and Clinical Research Center, Tanta University, Tanta, Egypt

Supplementary discussion

In composites of polymer matrix reinforced with filler particles interacting with each other, the shear modulus E' can be calculated according to Takayanagi's model¹ using Eq. (S1);

$$E' = \frac{(1 - 2\phi + \phi X_r)E_s E_r + (1 - X_r)\phi E_r^2}{(1 - X_r)E_r + (X_r - \phi)E_s} \quad (S1)$$

with ϕ being the volume fraction of reinforcing filler participating in the stress-transfer. The X_r is volume fraction of filler in composite. E_s and E_r are the shear moduli of the neat polymer matrix and the filler respectively.

In case of EO-EPI/CNC nanocomposite, when the stiffness of CNCs filler is much higher than EO-EPI matrix, Eq. (S1) can be simplified as;

$$E' = \phi E_r \quad (S2)$$

in which the volume fraction of the CNC, ϕ can be expressed as²;

$$\phi = \begin{cases} 0, & X_r < X_c \\ X_r \left(\frac{X_r - X_c}{1 - X_c} \right)^b, & X_r > X_c \end{cases} \quad (S3)$$

The critical percolation exponent is defined by b and the critical CNC percolation volume fraction (percolation threshold) is defined by X_c , which related to aspect ratio A of CNCs by $X_c = 0.7/A$. The parameters used to fit the experimental data against the percolation model shown in **Figure 5** include EO-EPI matrix tensile storage modulus of 2.9 MPa, a percolation exponent of

0.4, cotton-CNC aspect ratio A of 11 and E_r of 0.34 GPa, tunicate-CNC aspect ratio A of 76 and E_r of 6.41 GPa.

Table S1. Composition and tensile storage moduli of the EO-EPI/CNC and EO-EPI/PVA/CNC nanocomposites studied.^a

Composition	Storage Modulus, E' (MPa)	
	At -60 °C	At 25 °C
EO-EPI/2.5%CNC	3943 ± 211	3.5 ± 0.2
EO-EPI/5%CNC	4790 ± 218	5.3 ± 0.6
EO-EPI/6%CNC	4172 ± 234	5.5 ± 0.8
EO-EPI/7%CNC	4428 ± 593	19.9 ± 0.8
EO-EPI/9%CNC	4268 ± 488	25.0 ± 5.7
EO-EPI/10%CNC	5314 ± 353	50.0 ± 4.0
EO-EPI/5%PVA/1%CNC	3509 ± 194	2.2 ± 0.3
EO-EPI/5%PVA/2.5%CNC	4512 ± 358	4.0 ± 0.7
EO-EPI/5%PVA/5%CNC	4592 ± 53	5.3 ± 0.6
EO-EPI/5%PVA/6%CNC	5634 ± 664	5.9 ± 0.7
EO-EPI/5%PVA/7%CNC	4135 ± 410	21.3 ± 1.5
EO-EPI/5%PVA/9%CNC	4928 ± 550	29.8 ± 2.4
EO-EPI/5%PVA/10%CNC	5800 ± 231	206 ± 16
EO-EPI/5%PVA/15%CNC	7691 ± 10	230 ± 13
EO-EPI/5%PVA/20%CNC	6806 ± 378	251 ± 24

^aData were acquired from DMA analyses and represent averages of N = 3–5 individual measurement, ± standard deviation.

a)



b)

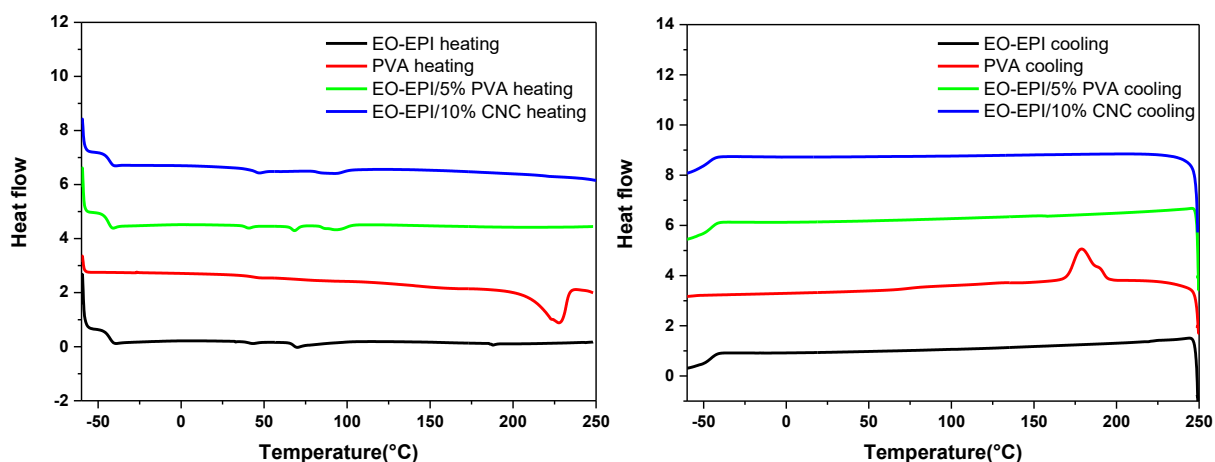


Figure S1. a) Pictures of EO-EPI/PVA blends with a PVA content of 0, 5, 10, 15 or 20% w/w respectively (from left). b) Differential scanning calorimetry thermograms (left: first heating, right: first cooling) of neat EO-EPI, neat PVA, a blend of EO-EPI and 5% w/w PVA, and a nanocomposite of EO-EPI with 10% w/w CNCs.

Table S2. Enthalpy of melting and degree of crystallinity of neat EO-EPI, a blend of EO-EPI and 5% w/w PVA, and a nanocomposite of EO-EPI with 10% w/w CNC.

Composition	Enthalpy of melting,	
	ΔH_m (J/g)	Degree of crystallinity, X_c^a (%)
Neat EO-EPI	3.66	1.6
EO-EPI/5%PVA	3.77	1.7
EO-EPI/10%CNC	3.45	1.6

^a calculated taking PEO as the 100% crystalline reference

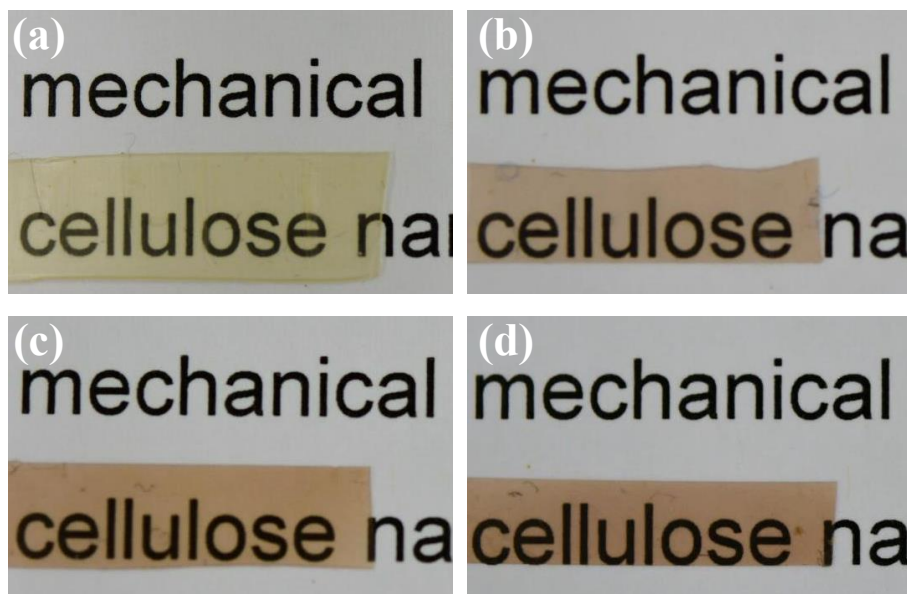


Figure S2. Pictures of EO-EPI/CNC/PVA nanocomposite films containing 10% w/w CNCs and (a) 0% w/w, (b) 1% w/w, (c) 3% w/w, or (d) 5% w/w of PVA.

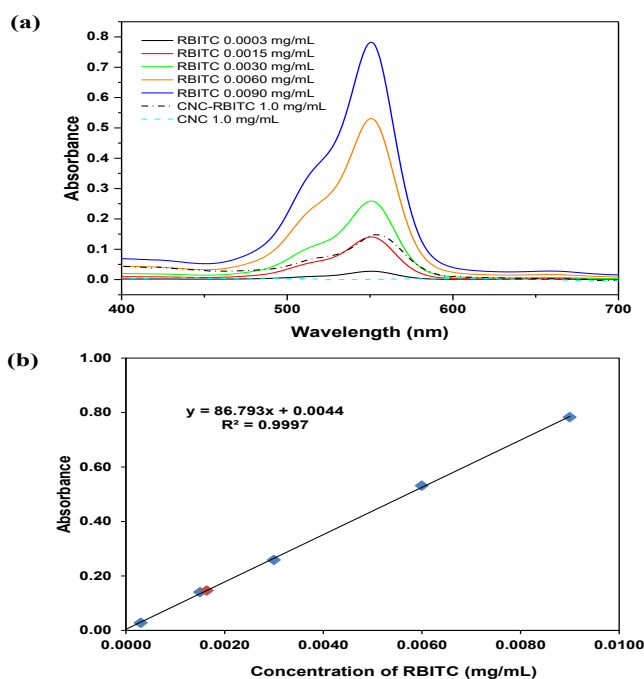


Figure S3. a) UV-Vis absorbance spectra of an aqueous suspension of unlabeled CNCs (1.0 mg/mL), an aqueous suspension of rhodamine-labelled CNCs (1.0 mg/mL) and solutions of free RBITC in water (0.0003-0.0090 mg/mL). b) Plot showing the UV-Vis absorption of the samples in (a) at a wavelength of 550 nm against the concentration of RBITC solutions. The value at the intercept of the resulting graph with the x-axis was used as the amount of rhodamine on the CNC.

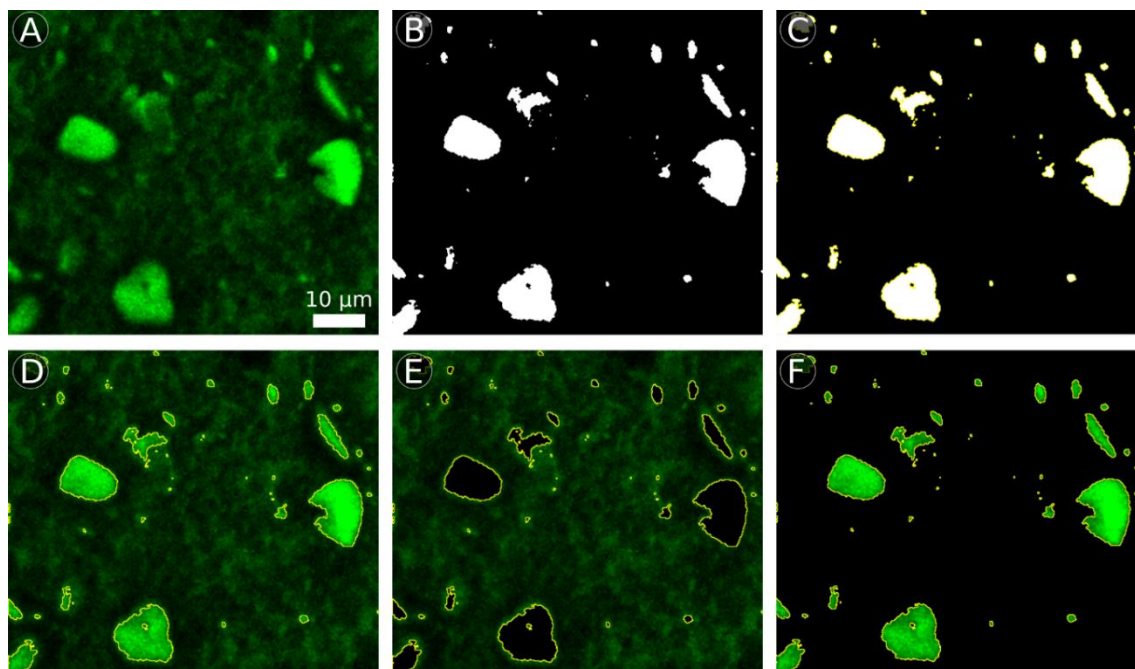


Figure S4. a) The raw dataset. The image shows clusters of pixels with a high intensity on a background of pixels at a lower intensity. b) Masking. The result of the ISOData (Iterative Self-Organizing Data Analysis Technique Algorithm) algorithm is pixel classification of the image into Pixels with Intensities Above the Threshold, PIAT (white) and Pixels with Intensities Below the Threshold, PIBT (black). The algorithm adjusts the number of clusters automatically during the iteration by merging similar clusters and splitting clusters with large standard deviations. The threshold is corrected dynamically until the variation between the two clusters is minimized. c) Selection. The mask can be converted into a selection of pixels, from which values can be retrieved. The selection unites the pixels with intensities higher than the dynamically established threshold. d) Overlay of the raw data with the selection. The overlay shows that the high intensity regions in the network were selected. e) Overlay of the raw data with inverse selection. By inverting the selection of PIAT, the PIBT can be selected. Here, the PIAT are removed (black). f) Overlay of the raw data with selection. The PIAT are shown, while the PIBT are removed (black).

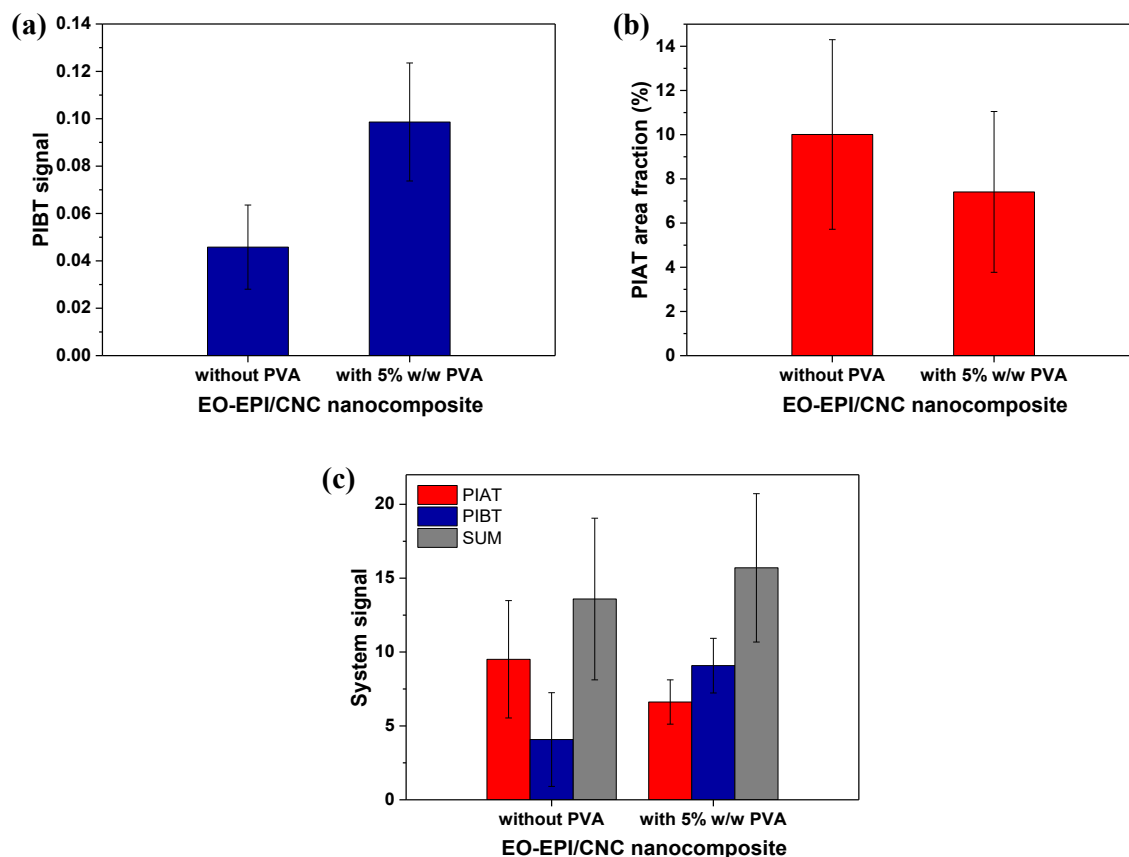


Figure S5. (a) Relative contribution of the pixels with intensities below threshold (PIBT) to the total signal. The relative intensity increase, an indication of more network components in the PIBT and less in the pixels with intensities below threshold (PIAT), upon addition of 5% w/w PVA is significant ($p \ll 0.001$). (b) Area fraction covered by pixels with intensities above the threshold. The decrease of high intensity PIBT, again an indication of network components moving from PIAT to PIBT, upon addition of 5% w/w PVA is significant ($p = 0.02$). (c) These two effects combined yield, upon addition of 5% w/w PVA, a net effect of less signal originating from the PIAT (red bars) while more signal is originating from PIBT (blue bars). Combined (grey bars), a slightly higher signal is measured, which can be attributed to quenching in the PIAT. Moreover, a clear and significant ($p \ll 0.001$) shift from a PIAT dominated signal (red bars) to a PIBT dominated signal (blue bars) can be observed.

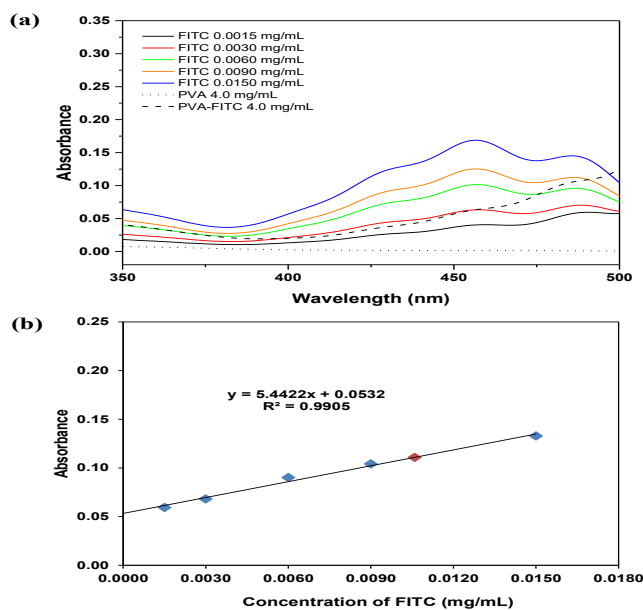


Figure S6. a) UV-Vis absorbance spectra of a solution of 4.0 mg/mL unlabeled PVA, a solution of 4.0 mg/mL fluorescein-labelled PVA and solutions of free FITC in DMSO (0.0015-0.0150 mg/mL). b) Determining the concentration of fluorescein on PVA by plotting UV-Vis absorption at a wavelength of 490 nm against concentration of FITC solutions. The value at the intercept of the resulting graph with the x-axis was used as the amount of fluorescein on the PVA.

References

1. Takayanagi, M.; Uemura, S.; Minami, S. Application of Equivalent Model Method to Dynamic Rheo-Optical Properties of Crystalline Polymer. *Journal of Polymer Science Part C: Polymer Symposia* **1964**, 5, 113-122.
2. Ouali, N.; Cavaille, J. Y.; Perez, J. Elastic, Viscoelastic and Plastic Behavior of Multiphase Polymer Blends. *Plastics, Rubber and Composites Processing Applications* **1991**, 55-